Journal of Materials Chemistry A

PAPER

View Article Online
View Journal | View Issue

Cite this: J. Mater. Chem. A, 2014, 2, 12770

One-step synthesis of hollow $Cr(OH)_3$ micro/nano-hexagonal pellets and the catalytic properties of hollow Cr_2O_3 structures†

Y. K. Bai,‡[ac] R. T. Zheng,‡*[a] Q. Gu,[a] J. J. Wang,[b] B. S. Wang,[a] G. A. Cheng[a] and G. Chen[b]

Received 27th February 2014
Accepted 23rd May 2014

DOI: 10.1039/c4ta00999a

www.rsc.org/MaterialsA

Novel $Cr(OH)_3$ hollow hexagonal pellets are synthesized at room temperature based on the chemical reaction between $CrCl_3$ and $NaBH_4$ in aqueous solution without any templates and surfactants. The evolution of the products obtained at different reaction times revealed that the hollow structure was formed *via* an orientation self-assembly and selective-etching process. The size and shape of the $Cr(OH)_3$ hollow hexagonal pellets can be adjusted by changing the reaction conditions. Annealing these $Cr(OH)_3$ hollow pellets at high temperatures convert them into Cr_2O_3 hollow structures, which are demonstrated in this paper to exhibit better catalytic performance than conventional Cr_2O_3 nanoparticles in the dehydrogenation of isobutane. This template-free and surfactant-free method enables low cost and high yield synthesis of hollow micro/nanostructures.

Introduction

Over the past decade, inorganic hollow micro/nanostructures have attracted lots of interest[1,2] for applications in energy-storage,[3,4] catalysis,[5] sensing,[6,7] drug delivery,[8–11] and photonics.[12,13] Template-based methods have been the most popular process for synthesizing hollow structures,[14–16] but the complicated process limits the application of this method. Different strategies such as the Kirkendall effect,[17,18] Ostwald ripening,[19–21] galvanic replacement,[22,23] surface-protected etching[24] and water-soluble salt templates[25–27] have been developed to simplify the synthesis process. However, the Kirkendall effect or Ostwald ripening based methods cost a lot of time, energy and capital. Galvanic replacement and water-soluble template methods still require templating. The surface-protected etching process can be carried out at room temperature without additional templates, but it still needs a surface protecting agent to create an etching rate difference between the inner part and the outer part of the solid sphere. Methods to synthesize hollow micro/nanostructures with good size and shape control, high yields, low cost and good reproducibility are desirable.

Chromium oxides have been extensively investigated because of their possible industrial application in catalysts, solar energy collectors, corrosion-resistant coating and nonreciprocal optical properties.[28,29] Nano- or micro-chromium oxide spheres could be prepared by heating uniform sized $Cr(OH)_3$ spheres, which are easy to obtain by a hydrolysis process.[30] Compared with spheres, hollow micro/nanostructures are more attractive because of their higher specific area. In this paper, we report the fabrication of $Cr(OH)_3$ micro/nano hollow hexagonal pellets *via* a room temperature one-step inorganic chemical synthesis. We further investigated the catalytic properties of Cr(III) hollow structures, and found that the hollow structure exhibits higher conversion efficiency during the oxidative dehydrogenation of ethane.

Experimental section

Material preparation

Chromium chloride hexahydrate ($CrCl_3 \cdot 6H_2O$, 98%), sodium borohydride ($NaBH_4$, 98%), sodium hydroxide (NaOH, 50% w/w aqueous solution), and deionized water were all purchased from Alfa Aesar and used as bought.

Hollow $Cr(OH)_3$ hexagonal pellets were prepared by the reaction of $CrCl_3$ with $NaBH_4$ at room temperature. Typically, 0.164 g $CrCl_3 \cdot 6H_2O$ was dissolved in 50 ml H_2O to form a dark green solution A, and 0.064 g $NaBH_4$ was dissolved in 50 ml H_2O to form a colorless transparent solution B. Then we poured solution B into solution A under vigorous stirring. The color of the solution changed from green to light blue immediately.

[a]Key Laboratory of Radiation Beam Technology and Materials Modification of Ministry of Education, College of Nuclear Science and Technology, Beijing Normal University, Beijing 100875, P. R. China. E-mail: rtzheng@bnu.edu.cn

[b]Department of Mechanical Engineering, Massachusetts Institute of Technology, 77 Massachusetts Avenue, Cambridge, Massachusetts 02139, USA

[c]Key Laboratory of Advanced Materials sponsored by the Ministry of Education of China, School of Materials Science and Engineering, Tsinghua University, Beijing 100084, P. R. China

† Electronic supplementary information (ESI) available. See DOI: 10.1039/c4ta00999a

‡ These authors contributed equally to this work.

After 15 minutes, there were no bubbles generated in the solution, indicating that the reaction was complete. The particle size of $Cr(OH)_3$ hexagonal boxes was tuned by adjusting pH in the solution with NaOH. The as-prepared products were centrifuged from the solution at 6000 rpm for 15 min. The derived products were washed with ethanol three times to obtain the light blue reaction products. The dark green Cr_2O_3 hexagonal hollow boxes were obtained by annealing the $Cr(OH)_3$ hexagonal drums at 450 °C for 30 minutes.

Material characterization

Crystal structures of the hollow $Cr(OH)_3$ hexagonal pellets and hollow Cr_2O_3 boxes were identified using a powder X-ray diffractometer (XRD) (Rigaku RU300, Japan), employing Cu-Kα radiation (λ = 1.5418 Å) at 50 kV and 300 mA. The sizes and morphologies of the $Cr(OH)_3$ and Cr_2O_3 hollow structures were observed by field emission scanning electron microscopy (FE-SEM) (Hitachi S-4800, Japan) at 10 kV and transmission electron microscopy (TEM) (JEOL Ltd. JEM-2010, Japan) at 200 kV. For the TEM and SEM measurements, the suspension was dropped onto aluminum foil paper and a high-resolution micro-grid, respectively, followed by air drying. The average particle size of the hexagonal particles was measured using a Zetasizer Nano ZS90 (Malvern Instruments). And the BET surface area value was measured using an automated gas sorption analyzer (Quantachrome Corporation).

The catalytic performance tests were conducted in a fixed-bed flow type quartz reactor packed with 0.15 g of the catalyst and 1 g of quartz sand at atmospheric pressure. The reactant stream consisting of 60% carbon dioxide, 20% isobutane, and 20% Ar was introduced into the reactor at a flow rate of 2000 ml h^{-1} g^{-1}. The reaction temperature was varied from 773 K to 973 K. The products were online analyzed by gas chromatography (Shimadzu GC-2014, Japan) with a double column dual-detector. The hydrocarbon product was detected using a flame ionization detector (FID) through the Al_2O_3 capillary column. CO and CO_2 are detected using a thermal conductivity detector (TCD) through the GDX-502 packed column. The catalytic performance of nanostructured-Cr_2O_3 for oxidative dehydrogenation of isobutane with CO_2 was compared with that of the normal nano-Cr_2O_3 catalyst which was commercially available.

The conversion, yield and selectivity were calculated by the following equations:

$$\text{Conversion } (\%) = (n_g/(n_{ba} + n_g)) \times 100$$

$$\text{Yield } (\%) = (n_{be}/(n_{ba} + n_g)) \times 100$$

$$\text{Selectivity } (\%) = (n_e/n_g) \times 100$$

where n_{be} and n_{ba} are the number of moles of isobutene and isobutane at the exit of the reactor, respectively, n_g is the number of moles of isobutane converted into the gaseous products (isobutene, propane, propene, ethane, ethene and methane) and n_e is the number of moles of alkene (isobutene, propene, ethene) converted from isobutane. The calculations do not consider the conversion of isobutane to coke, as its instantaneous formation is time dependent and difficult to estimate.

Results and discussion

$Cr(OH)_3$ hexagonal pellets were obtained by a reaction of aqueous chromium chloride ($CrCl_3$) solution and aqueous sodium borohydride ($NaBH_4$) solution at room temperature. Typically, a 50 ml 12.3 mM $CrCl_3$ solution is poured into a 50 ml 33.7 mM $NaBH_4$ solution. The two solutions reacted vigorously and produced a large number of bubbles and a grey-green suspension. After 5 days of standing, the color of the suspension changed from grey-green to brilliant green. The as-prepared suspensions were centrifuged and washed with DI water three times to obtain the light blue reaction products. The crystallographic structure of the products was determined by powder X-ray diffraction (XRD). Fig. 1a shows the XRD pattern of the reaction product in the 2θ range of 10–80°. The pattern could be distinctly indexed to a hexagonal phase with lattice constants a = 5.288 Å, b = 4.871 Å for $Cr(OH)_3 \cdot 3H_2O$ (JCPDS no. 16-0817), revealing the crystalline nature of the product. It is worth noting that the peak intensity of diffraction peaks was low, indicating that $Cr(OH)_3$ is not well crystallized.

The scanning electron microscopy (SEM) image shows that the light blue precipitates are submicron-sized hexagonal pellets with six equilateral rectangular lateral surfaces and two hexagonal upper and lower surfaces (Fig. 1b). The pellets are uniform in size, the average side-length of the hexagon is about 300 nm, and the average height of the pellets is about 350 nm. The inset picture in Fig. 1b is a higher magnification SEM image

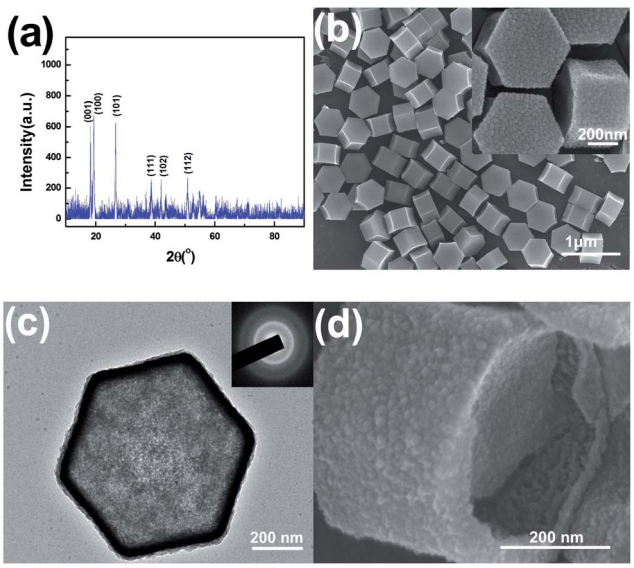

Fig. 1 The microstructure of hollow $Cr(OH)_3$ hexagonal pellets. (a) XRD patterns of the as-prepared products. (b) A SEM image of $Cr(OH)_3$ hexagonal pellets. The inset is a high magnification SEM image of $Cr(OH)_3$ hexagonal pellets. (c) A TEM image of the as-prepared $Cr(OH)_3$ hexagonal pellets, which shows the hollow nature of the hexagonal pellets. The inset is the SAED pattern of the hollow $Cr(OH)_3$ hexagonal pellet. (d) A SEM image of a broken hollow $Cr(OH)_3$ hexagonal pellet.

of the products. It could be observed that the surfaces of these pellets are covered with 20–30 nm diameter particles. Transmission electron microscopy (TEM) images provide further insight into the structure of the obtained $Cr(OH)_3$ hexagonal pellets, as shown in Fig. 1c. It is found that the $Cr(OH)_3$ hexagonal pellet has a hexagonal hollow interior and high geometrical symmetry: with identical angles between two adjacent rectangular surfaces and parallel top and bottom surfaces. The thickness of the wall is about 40 nm. The diffuse halos in the selected area electron diffraction (SAED) pattern (the inset picture in Fig. 1c) indicate the amorphous nature of these hexagonal pellets, which is inconsistent with the XRD results. According to our observation, $Cr(OH)_3 \cdot 3H_2O$ is unstable in a dry and hot environment, it could be very easily dehydrated and turned into an amorphous structure (Fig. S1, ESI†). We conjecture that the different results between XRD and SAED are due to the vacuum dehydration and electron radiolysis of TEM samples in the high vacuum chamber. Fig. 1d shows the SEM image of a broken $Cr(OH)_3$ hexagonal pellet. It is found that the inner surfaces of the hollow hexagonal pellets are very rough. It seems that the wall of hollow hexagonal pellets consists of aggregated nanoparticles.

To investigate the formation mechanism of $Cr(OH)_3$ hexagonal pellets, we drew up 2 ml of mixed solution using a pipette and dropped it into 50 ml anhydrous alcohol to stop the reaction after different times of reaction. The reaction products were then separated from the alcohol *via* an ultra-high speed centrifuge. Fig. 2 shows the microstructural evolution of the reaction products. At the beginning (1 s of reaction, Fig. 2a), a large number of irregular nanoparticles with a diameter of 20–35 nm were formed. After 3 s of reaction (Fig. 2b), a large number of hexagonal pellets appeared. The average side length of the hexagon is about 95 nm and the average height of the pellets is about 135 nm. The surfaces of the hexagonal pellets are rough and covered with 20–35 nm diameter particles. Besides pellets, a large number of nanoparticles with a diameter of 20–35 nm still could be observed. After 15 s of reaction (Fig. 2c), only hexagonal pellets could be observed. The size and morphology of the pellets are similar to those of the pellets shown in Fig. 2b. The yield of this solid product is 96.85%. One day later, the hexagonal pellets grow up. The average side length of the hexagon turns to be 129 nm and the average height of the pellets is about 183 nm. The surfaces of the hexagonal pellets become smooth and depressed, as shown in Fig. 2d. Meanwhile, XRD characterization (Fig. S2, ESI†) indicates that the hexagonal pellets begin to crystallize during the course. The TEM image (the inset in Fig. 2d) shows that cavities begin to appear in the interior of some pellets. From then on, the appearance of the hexagonal pellets changes a little, but their interior begins to change. Three days later, the hollowing process of the hexagonal pellets is continued. It could be observed from Fig. 2e that some pellets turn to be hollow structures, some pellets are half hollowing, and some pellets are still solid structures. Five days later, all the solid hexagonal pellets change into complete hollow structures, as shown in Fig. 2f. The detailed TEM image of the hollowing process is provided in the ESI† (Fig. S3). The yield of the hollow product in Fig. 2f is 58.18%.

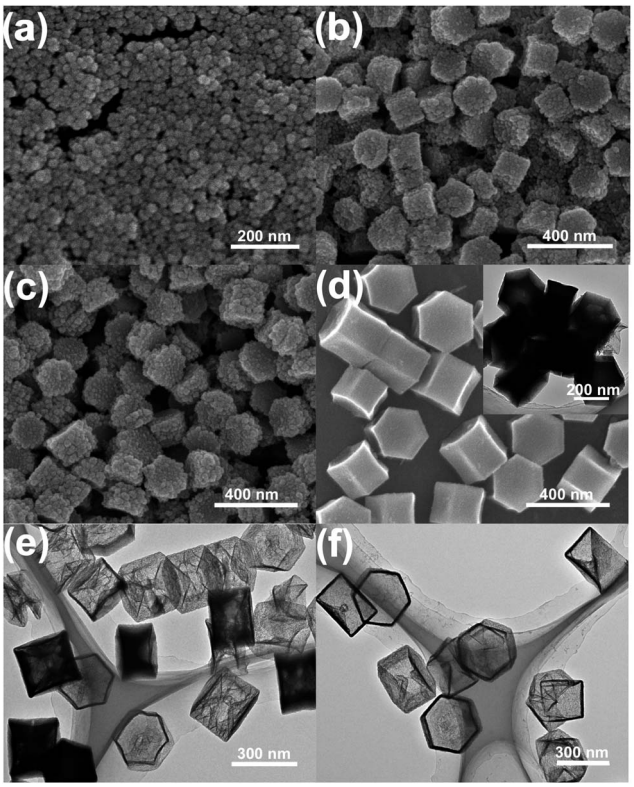

Fig. 2 Microstructural evolution of $Cr(OH)_3$ hexagonal pellets. (a) A SEM image of products after 1 second of reaction. (b) A SEM image of products after 3 seconds of reaction. (c) A SEM image of products after 15 seconds of reaction. (d) A SEM image of products after 1 day of reaction, the inset is a TEM image of the same products. (e) A TEM image of products after 3 days of reaction. (f) A TEM image of products after 5 days of reaction.

Based on the above experimental observations, we conjured that the hexagonal hollow pellets of $Cr(OH)_3$ are formed by the orientation self-assembly of nanoparticles and selective-etching of the pellet interior. Fig. 3 shows schematic illustration of the formation of the hollow microstructure. As reported in a previous study,[31] when $NaBH_4$ is added into water, it will react with water and forms BO_2^- ions and hydrogen. BO_2^- will further hydrolyze into $B(OH)_3$ and OH^-. When the $CrCl_3$ solutions are mixed with the $NaBH_4$ solutions, insoluble $Cr(OH)_3$ nanoparticles are precipitated from the solution. The reactions can be expressed as eqn (1)–(3).

$$BH_4^- + 2H_2O = BO_2^- + 4H_2\uparrow \quad (1)$$

$$BO_2^- + 2H_2O = B(OH)_3 + OH^- \quad (2)$$

$$Cr^{3+} + 3OH^- = Cr(OH)_3\downarrow \quad (3)$$

As shown in Fig. 2, $Cr(OH)_3$ hexagonal pellets were formed within a few seconds, it is hard to observe how these $Cr(OH)_3$ nanoparticles form submicron structures with regular geometric outlines. We suppose that the $Cr(OH)_3$ hexagonal pellets may be formed by the orientation self-assembly[32,33] of

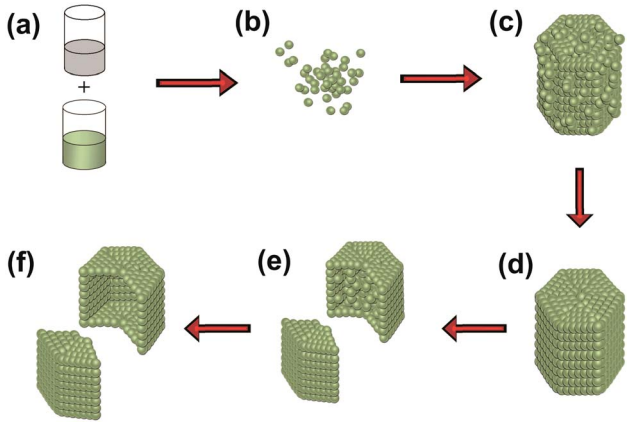

Fig. 3 Schematic illustration of the formation process of a hollow $Cr(OH)_3$ hexagonal pellet. (a) The $CrCl_3$ solution is mixed with the $NaBH_4$ solution. (b) $Cr(OH)_3$ nanoparticles form immediately. (c) Nanoparticles self-assemble into a $Cr(OH)_3$ hexagonal pellet. (d) Ostwald ripening and surface reconstruction of the hexagonal pellet. (e) H^+ ions penetrate into the $Cr(OH)_3$ hexagonal pellets and form cavities inside. (f) Hollow hexagonal pellet forms.

$Cr(OH)_3$ nanoparticles (Fig. 3b and c). After the $Cr(OH)_3$ hexagonal pellets are formed, their structures are relatively stable. However, the chemical reaction still continues. $B(OH)_3$ could hydrolyze and form $[B(OH)_4]^-$ and H^+. H^+ will react with $Cr(OH)_3$ and etch the surfaces of $Cr(OH)_3$ hexagonal pellets. At the same time, Cr^{3+} will also hydrolyze and precipitate $Cr(OH)_3$ again. Ostwald ripening and surface reconstruction take place in the next 24 hours to form the perfect hexagonal pellets with larger sizes and smoother surfaces (Fig. 3d). The reactions can be expressed as eqn (4) and (5).

$$B(OH)_3 + H_2O = [B(OH)_4]^- + H^+ \quad (4)$$

$$Cr(OH)_3 + 3H^+ \rightleftharpoons Cr^{3+} + 3H_2O \quad (5)$$

Meanwhile, small H^+ ions could also penetrate into the $Cr(OH)_3$ hexagonal pellets from the surface gaps, etch the interior part and form cavities inside the hexagonal pellets, as indicated in Fig. 3e. Cr^{3+} ions, the product of H^+ ions etching $Cr(OH)_3$ hexagonal pellets, will continuously hydrolyze and produce more and more H^+ ions.[34] Some H^+ ions could diffuse out of the particles, but most H^+ ions are kept in the cavities inside the hexagonal pellets. The concentration of H^+ ions in the cavities is higher than that in the solution, leading to a relatively higher etching rate within the pellets. Further etching removes the material from the core and produces a more pronounced hollow structure. After several days of etching, hollow $Cr(OH)_3$ hexagonal pellets are formed, as shown in Fig. 3f.

Obviously, the hollowing process is sensitive to the pH in the solution and the density of the particles. We found that too low pH will make hexagonal pellets etch from outside to inside (Fig. S4, ESI†). pH between 5 and 6 is beneficial to the hollowing of $Cr(OH)_3$ hexagonal pellets. A loose structure is helpful for reducing the etching time of a hollow $Cr(OH)_3$ hexagonal pellet. A hollow loose structure is obtained after 12 hours of reaction in our experiment (Fig. S5, ESI†).

The formation mechanism of hollow $Cr(OH)_3$ hexagonal pellets not only gives a simple one-step strategy for hollow structure synthesis, but also provides an opportunity to control the shape of hollow pellets. The shape of pellets is a function of the reactant concentration and stoichiometric proportion of reactants. The size and aspect ratio (height/(2 × side length)) of $Cr(OH)_3$ hexagonal pellets can be controlled by adjusting the reaction conditions. Fig. 4 shows the SEM images of $Cr(OH)_3$ hexagonal pellets obtained at different reaction conditions. It is observed that the average aspect ratios of pellets in Fig. 4a and b are about 0.55, similar to those in Fig. 1b, but the average side lengths of hexagonal pellets in Fig. 4a and b are 133 nm and 505 nm, respectively. We also obtained pellets having a similar side length to that in Fig. 1b (about 300 nm), but with the average aspect ratios of 0.43 (Fig. 4c) and 1.15 (Fig. 4d), respectively. The wall thickness of these hollow pellets can be controlled by the aging times, as shown in Fig. 2. We have also synthesized oblate spheres, donuts, nuts, tubes and other interesting micro/nanostructures besides hollow hexagonal pellets by this simple and cheap synthesis strategy (Fig. S6, ESI†). Vivid $Cr(OH)_3$ nanostructures are candidates for different potential applications.

Cr_2O_3-based catalysts have been proved active for the dehydrogenation of alkanes. Dehydrogenation of ethane, propane and isobutane has become an important route to satisfy the increasing demand for light olefins at present.[35–37] The dehydrogenation of isobutane by the unconventional oxidant CO_2 has attracted interest from scientists and engineers because CO_2 could inhibit some of the side reactions such as coking and cracking,[38–41] which has been proved in our experiments too

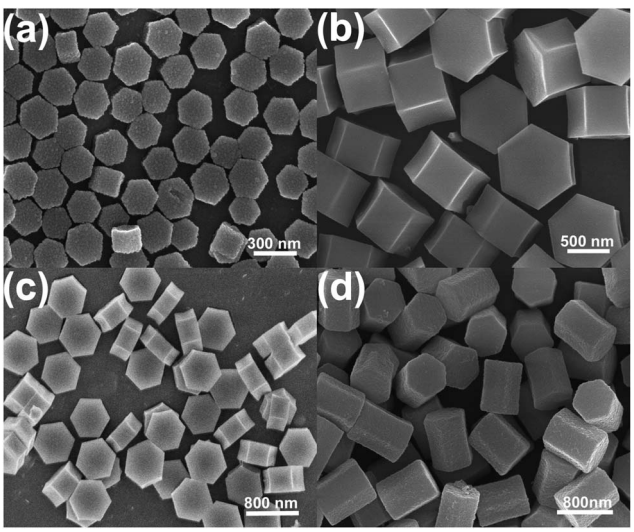

Fig. 4 SEM images of products obtained at different reaction conditions after 3 days of reaction. (a) 50 ml 11.25 mM $CrCl_3$ solution react with 50 ml 19.6 mM $NaBH_4$ solution. (b) 50 ml 11.25 mM $CrCl_3$ solution react with 50 ml 22.4 mM $NaBH_4$ solution. (c) 50 ml 15.39 mM $CrCl_3$ solution react with 50 ml 30.5 mM $NaBH_4$ solution. (d) 50 ml 1.2 mM $CrCl_3$ solution react with 50 ml 3.2 mM $NaBH_4$ solution.

(Fig. S7, ESI†). The total reaction equation can be expressed as eqn (6).[42]

$$\text{i-}C_4H_{10} + CO_2 \rightleftharpoons \text{i-}C_4H_8 + CO + H_2O \quad (6)$$

Compared with solid particles, Cr_2O_3 hollow pellets have a larger specific surface area, and should have higher catalytic efficiency. Hollow Cr_2O_3 pellets were obtained by the annealing of hollow $Cr(OH)_3$ hexagonal pellets. We prepared four kinds of hollow $Cr(OH)_3$ hexagonal pellets with a similar aspect ratio (0.75), a similar wall thickness (~40 nm) and different sizes. The average height of each pellet is 203, 284, 396 and 510 nm, respectively. The $Cr(OH)_3$ hexagonal pellets were annealed at 620 °C for 30 minutes, and a dark green product was obtained. XRD patterns (Fig. 5a) of the annealed product indicate that the original $Cr(OH)_3$ is changed into Cr_2O_3 (JCPDS no. 38-1479). SEM images show that these dark green products are hexagonal hollow boxes with porous and rough surfaces (Fig. 5b).

Fig. 5c and d show the isobutane conversion rate and alkene selectivity as a function of temperature. The conversion and selectivity of isobutane were defined as in previous research.[43] In addition to the Cr_2O_3 hollow structures with different average particle sizes, commercial Cr_2O_3 nanoparticles (particle size: 60 nm, bought from Adamas-beta, Switzerland) were also tested for comparison. The amount of Cr_2O_3 hollow structures and commercial Cr_2O_3 nanoparticles for all tests is 0.15 g.

Experimental results (Fig. 5c) indicated the isobutane conversion as a function of temperature between 773 K and 973 K. From 853 K to 883 K, the isobutane conversions improve remarkably, especially for those Cr_2O_3 hollow catalysts. Moreover, the smaller the Cr_2O_3 hollow structure is, the better catalytic behavior it has. At 883 K, the Cr_2O_3 hollow structure with an average size of 203 nm (Cr 203) shows the best conversion (86%) among all catalysts, while Cr_2O_3 nanoparticles only exhibit a conversion of 60%. This is not only because the smaller hollow Cr_2O_3 has a larger specific surface area (ESI,† Table S1), but also due to the fact that hollow Cr_2O_3 particles agglomerate less than Cr_2O_3 nanoparticles. From 883 K to 913 K, the isobutane conversions in the reactor with a small Cr_2O_3 catalyst (Cr 203, Cr 284, Cr 396, Cr nano) decreased, which may due to the growth of the Cr_2O_3 grain. The conversion of isobutane increases when the temperature is higher than 913 K. We speculate that the reason is that the pyrolysis of isobutane became serious at high temperatures, because the hydrocarbon cracking process is an endothermic reaction.[44] Fig. 5d shows that the selectivity of Cr_2O_3 catalysts with different average heights (203 to 510 nm) and commercial purchased nano-Cr_2O_3 particles has a peak at 853 K, the selectivity of the hollow Cr_2O_3 catalyst with an average height of 284 nm reaches 70% at 853 K. The varying trend of selectivity is different from that of conversion. Isobutene is easy to further degrade into methane, a larger surface area could decrease the alkene selectivity at high temperatures. According to the definition of selectivity, it may result in the selectivity peak at 853 K. Considering the balance of cost and catalytic efficiency, 883 K is an optimal working temperature for these hollow Cr_2O_3 catalysts. In previous research, it was found that the selectivity of Cr_2O_3 could be improved by doping other metal oxides such as Zr, Ce, and Ca.[45–47] By an appropriate doping process, we believe that the hollow Cr_2O_3 catalyst could provide considerable isobutane conversion and alkene selectivity.

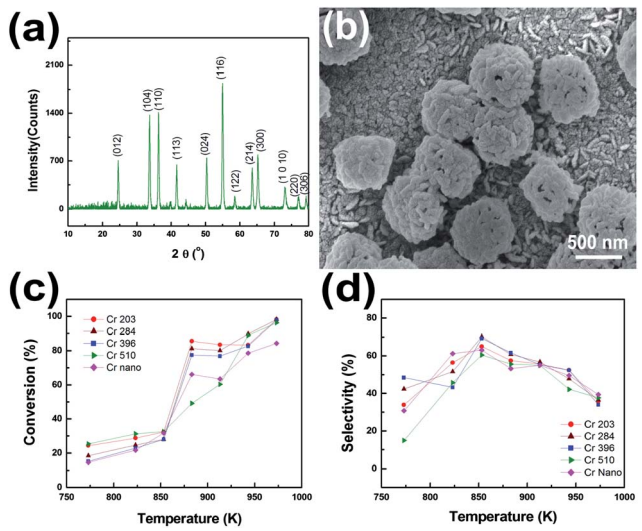

Fig. 5 Microstructure and the catalytic performance of the Cr_2O_3 hollow structures. (a) XRD patterns of the annealed product. (b) SEM images of the Cr_2O_3 hollow structure. (c) Conversion of i-C_4H_{10} as a function of temperature. (d) Alkene selectivity of i-C_4H_{10} dehydrogenation at different temperatures, in which Cr 203, Cr 284, Cr 396, and Cr 510 mean Cr_2O_3 hollow catalysts with an average height of 203 nm, 284 nm, 396 nm and 510 nm, respectively. Cr nano means commercial purchased nano-Cr_2O_3 particles.

Conclusions

In summary, we provide a one-step chemical reaction to synthesize hollow structures with a high yield and low cost. These hollow structures form through orientation self-assembly of nanoparticles and selective-etching of the pellet interior. By adjusting the reaction conditions, hollow $Cr(OH)_3$ hexagonal pellets with different sizes and aspect ratios were synthesized. Our synthesis simplifies the synthetic process of hollow structures. Hollow Cr_2O_3 hexagonal pellets were obtained by annealing the hollow $Cr(OH)_3$ hexagonal pellets. Smaller Cr_2O_3 hollow pellets have been proved to be more efficient for the dehydrogenation of isobutane. At 883 K, a Cr_2O_3 hollow structure with an average size of 200 nm has a conversion of 86%.

Acknowledgements

This work is supported by the Program for New Century Excellent Talents in University (NCET-11-0043), the National Basic Research Program of China (2010CB832905), the Fundamental Research Funds for the Central Universities, and AFOSR FA9550-11-1-0174 (G.C.). We would like to thank Prof. Z. Ren, Prof. Huiquan Li and Prof. Haitao Liu for their helpful discussion during this work.

References

1 A. D. Dinsmore, M. F. Hsu, M. G. Nikolaides, M. Marquez, A. R. Bausch and D. A. Weitz, *Science*, 2002, **298**, 1006.
2 J. P. Tian, Y. Zhou, Z. D. Li, Q. Liu and Z. G. Zou, *J. Mater. Chem. A*, 2013, **1**, 3575.
3 N. Venugopal, D. J. Lee, Y. J. Lee and Y. K. Sun, *J. Mater. Chem. A*, 2013, **1**, 13164.
4 X. W. Lou and L. A. Archer, *Adv. Mater.*, 2008, **20**, 1853.
5 H. Gu, J. N. Wang, Y. C. Ji, Z. Q. Wang, W. Chen and X. Gi, *J. Mater. Chem. A*, 2013, **1**, 12471.
6 S. Ikeda, S. Ishino, T. Harada, N. Okamoto, T. Sakata, H. Mori, S. Kuwabata, T. Torimoto and M. Matsumura, *Angew. Chem., Int. Ed.*, 2006, **45**, 7063.
7 P. Sun, X. Zhou, C. Wang, K. Shimanoe, G. Y. Lu and N. Yamazoe, *J. Mater. Chem. A*, 2014, **2**, 1302.
8 J. Liu, S. Z. Qiao, J. S. Chen, X. W. Lou, X. R. Xing and G. Q. Lu, *Chem. Commun.*, 2011, **47**, 12578.
9 J. F. Chen, H. M. Ding, J. X. Wang and L. Shao, *Biomaterials*, 2004, **25**, 723.
10 Y. F. Zhu, J. L. Shi, W. H. Shen, X. P. Dong, J. W. Feng, M. L. Ruan and Y. S. Li, *Angew. Chem., Int. Ed.*, 2005, **44**, 5083.
11 Q. J. He and J. L. Shi, *J. Mater. Chem.*, 2011, **21**, 5845.
12 Q. H. Cui, Y. S. Zhao and J. N. Yao, *J. Mater. Chem.*, 2012, **22**, 4136.
13 X. Xu and S. A. Asher, *J. Am. Chem. Soc.*, 2004, **126**, 7940.
14 R. Tenne and C. N. R. Rao, *Philos. Trans. R. Soc., A*, 2004, **362**, 2099.
15 K. J. C. Bommel, A. Friggeri, S. Shinkai, K. J. C. Bommel, A. Friggeri and S. Shinkai, *Angew. Chem., Int. Ed.*, 2003, **42**, 980.
16 X. W. Lou, L. A. Archer and Z. Yang, *Adv. Mater.*, 2008, **20**, 3987.
17 Y. D. Yin, R. M. Rioux, C. K. Erdonmez, S. Hughes, G. A. Somorjai and A. P. Alivisatos, *Science*, 2004, **304**, 711.
18 J. Yang, L. Qi, C. Lu, J. Ma and H. Cheng, *Angew. Chem., Int. Ed.*, 2005, **44**, 598.
19 H. G. Yang and H. C. Zeng, *Angew. Chem., Int. Ed.*, 2004, **43**, 5206.
20 H. C. Zeng, *J. Mater. Chem. A*, 2011, **21**, 7511.
21 X. W. Lou, Y. Wang, C. Yuan, J. Y. Lee and L. A. Archer, *Adv. Mater.*, 2006, **18**, 2325.
22 Y. G. Sun and Y. N. Xia, *Science*, 2002, **298**, 2176.
23 Y. Sun, B. Mayers and Y. Xia, *Adv. Mater.*, 2003, **15**, 641.
24 Q. Zhang, T. Zhang, J. Ge and Y. Yin, *Nano Lett.*, 2008, **8**, 2867.
25 X. W. Lou, C. Yuan, Q. Zhang and L. A. Archer, *Angew. Chem., Int. Ed.*, 2006, **45**, 3825.
26 M. R. Kim and D. J. Jang, *Chem. Commun.*, 2008, **41**, 5218.
27 Y. C. Pu, J. R. Hwu, W. C. Su, D. B. Shieh, Y. Tzeng and C. S. Yeh, *J. Am. Chem. Soc.*, 2006, **128**, 11606.
28 J. G. Morales, J. G. Carmona, R. R. Clemente and D. Muraviev, *Langmuir*, 2003, **19**, 9110.
29 H. Xu, T. Lou and Y. Li, *Inorg. Chem. Commun.*, 2004, **7**, 666.
30 M. J. Avena, C. E. Giacomelli and C. P. De Pauli, *J. Colloid Interface Sci.*, 1996, **180**, 428.
31 M. J. F. Ferreira, C. M. Rangel and A. M. F. R. Pinto, *Int. J. Hydrogen Energy*, 2012, **37**, 6985.
32 G. M. Whitesides and B. Grzybowski, *Science*, 2002, **295**, 2418.
33 M. Rycenga, P. H. C. Camargo and Y. Xia, *Soft Matter*, 2009, **5**, 1129.
34 H. Stunzi and W. Marty, *Inorg. Chem.*, 1983, **33**, 2145.
35 D. Shee and A. Sayari, *Appl. Catal., A*, 2010, **389**, 155.
36 B. Y. Jibril, A. Y. Atta, K. Melghit, Z. M. El-Hadi and A. H. Al-Muhtaseb, *Chem. Eng. J.*, 2012, **193**, 391.
37 O. Michitaka, I. Yoshihiro and I. Akira, *Appl. Catal., A*, 2004, **258**, 153.
38 J. F. Ding, Z. F. Qin, S. W. Chen, X. K. Li, G. F. Wang and J. G. Wang, *J. Fuel Chem. Technol.*, 2010, **38**, 458.
39 Y. W. Zhang, Y. M. Zhou, L. H. Wan, M. W. Xue, Y. Z. Duan and X. Liu, *Fuel Process. Technol.*, 2011, **92**, 1632.
40 D. R. Sergio, F. Giovanni, F. Silvia, I. Valerio and C. Alessandro, *Appl. Catal., A*, 1993, **106**, 125.
41 J. F. Ding, Z. F. Qin, X. K. Li, G. F. Wang and J. G. Wang, *Chinese Chem. Lett.*, 2008, **19**, 1059.
42 B. Y. Jibril, N. O. Elbashir, S. M. Al-Zahrani and A. E. Abasaeed, *Chem. Eng. Process.*, 2005, **44**, 835.
43 N. O. Elbashir, S. M. Al-Zahrani, A. E. Abasaeed and M. Abdulwahed, *Chem. Eng. Process.*, 2003, **42**, 817.
44 F. Gutiérrez and F. Méndez, *Energy Convers. Manage.*, 2012, **55**, 1.
45 S. Deng, H. Q. Li, S. G. Li and Y. Zhang, *J. Mol. Catal. A: Chem.*, 2007, **268**, 169.
46 P. Moriceau, B. Grzybowska, Y. Barbaux, G. Wrobel and G. Hecquet, *Appl. Catal., A*, 1998, **168**, 269.
47 G. Neri, A. Pistone, S. De Rossi, E. Rombi, C. Milone and S. Galvagno, *Appl. Catal., A*, 2004, **260**, 75.